Remote Sensing the Plasma Flows Around the Heliopsheath and Consequences for the Shape of the Heliosphere

University of New Hampshire

H. Kucharek*, J. Park+, P. Isenberg*, E. Moebius*, N. Schwadron*

*University of New Hampshire, 8 College Road, Durham, NH, 03824, USA
+Goddard Space Flight Center, Greenbelt, MD 20771, USA

EGU2017-9828
X4.256

ABSTRACT:

Remote sensing IBEX observations of the interstellar gas flow in the inner heliosphere provide the most detailed information about the physical conditions of the surrounding interstellar medium and the interaction of this flow with the heliosheath. An excellent diagnostic tool to probe this interaction is the secondary component of the interstellar neutral gas flow that originates from charge exchange between primary interstellar neutrals and the plasma at the heliosheath. The interstellar plasma is diverted around the heliosphere, and the neutrals that are emitted from this flow through charge exchange carry information on the diverted flow. Therefore, IBEX-lo sky maps of secondary neutral He, O, and H fluxes contain information on the interstellar plasma flow patterns and thus the shape of the heliosphere. We use asymmetries apparent in these flux maps to infer flow patterns around the heliosphere and thus to determine the global shape of the heliosphere. Further, these asymmetries in sky maps at varying energies contain spectral information which may allow us to investigate regions of plasma heating and acceleration. Thus, we demonstrate a new and powerful tool for the remote sensing of plasma flows in the heliosheath.

INTRODUCTION:

There are several possible populations of heliospheric energetic neutral atoms (ENAs) generated at the various heliospheric interfaces, the inner heliosphere, outer heliosphere, and the termination shock (TS). Depending on where and how these ENAs are generated, they belong to different energy regimes. While interstellar neutral (ISN) flow through the heliospheric boundary mostly unimpeded, a substantial fraction of ISN H and O is filtered before reaching the TS through charge exchange with ambient plasma ions. Secondary ISN atoms are generated by charge exchange reaction between ISN atoms and interstellar ions outside the heliosheath, forming walls of H and O in front of the heliopause (HP). Another population results from solar wind ions which are decelerated across the termination shock, charge exchanging with the ISN atoms in the inner heliosheath. The resulting newborn neutral atoms may contribute to the lowest energy ENA population, ~100 eV. Some of the newborn ions undergo a second charge exchange with these ISN atoms creating a low energy ENA population (Malama et al. 2006). A third population is created in the supersonic solar wind. These ENAs escape from the heliosphere and undergo charge exchange with the interstellar plasma beyond the HP, creating pickup ions in the ambient interstellar medium ISM. These newborn pickup ions exchange charges with the ISN atoms producing the secondary ENAs.

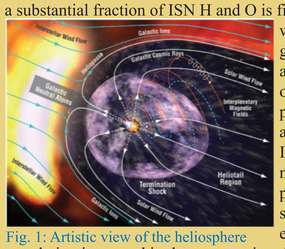

Fig. 1: Artistic view of the heliosphere

QUESTIONS & MOTIVATION:

The heliosphere can be compared with a obstacle in a flow of neutral and charge particles the flow pattern around it is determined by it's shape and the properties of the plasma/neutral flow.

Question: Can the IBEX-lo ENA maps be used as a tool to remotely sense the shape of the heliosphere ?

The flow around an obstacle is determined by its shape, the flow speed, and the temperature of the medium flowing around it. The flow speed is increasing when it is deflected and the pressure decreases. If the obstacle is the heliosphere this would impact the charge-exchange rate and thus the ENA signal. If this is true the ENA signal should contain information on the flow pattern around the heliosphere. Figure 2 shows a sketch of the flow around a sphere - numerical model and their predicted shape of the heliosphere are shown below:

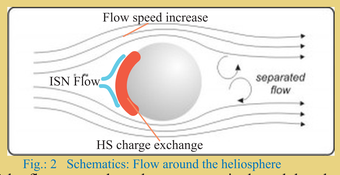

Fig.: 2 Schematics: Flow around the heliosphere

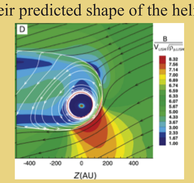

Izmodenov et al. 2015

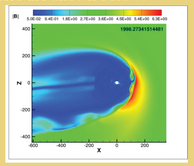

Pogorelov et al. 2015

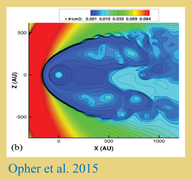

Opher et al. 2015

IBEX MEASUREMENT AND DATA ANALYSIS (Helium and Oxygen Sky Maps):

Previous studies of these data and sky maps have not fully analyzed them statistically. However, this is extremely important when studying heavy neutrals because the counting statistics will be relatively low. In order to analyze the data/sky maps we use three different statistical methods. **The data selection process includes the follwing steps:**

(1) "Good time selection": eliminates all effects from the inner heliosphere:
(2) "Sputter correction": Helium can only be detected indirectly by sputtered products. Oxygen also sputters hydrogen.
(3) "Statistical analysis":

Figures 3,4 show the results of the statistical analysis for Oxygen in energy step 5 (280eV):

Signal to Noise Filter:

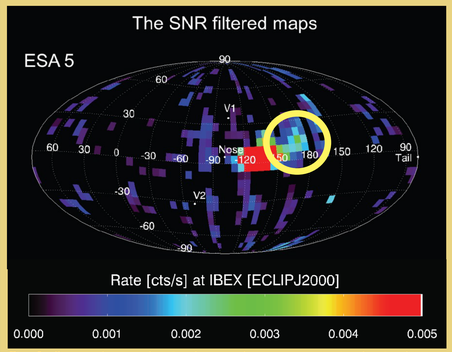

Fig.: 3 Oxygen sky map showing the secondary component using the signal to noise filter

Confidence Level Method:

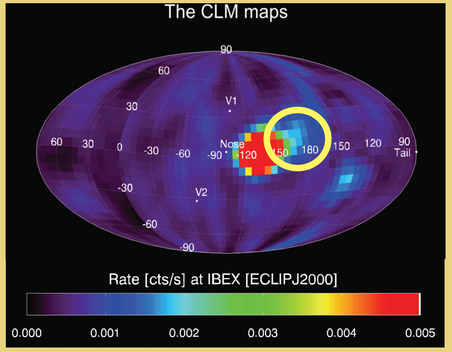

Fig.: 4 Oxygen sky map showing the secondary component using the confidence level method.

As a third method we used the Cluster analysis method, which is commonly used for low counting statistics. The extended feature (yellow circle) is reproduced in all three methods. Therefor, the likelihood of a real signal is very high. This feature has been identified as the secondary component (Park et al., 2015) which is created by the charge-exchange process in the heliosheath. This secondary component may contain information about the curvature of the heliosheath and thus of the heliosphere. However, a better candidate for this investigation is the helium ENA component.

SPUTTER CORRECTION & SECONDARY HELIUM COMPONENT:

The secondary neutral helium component would be expected in the energy range of 10-110eV. At this energy range sputtered hydrogen from hydrogen and oxygen ENA can be neglected. Thus helium can be determined by investigating the ENA spectrum from hydrogen. Figure 5 shows a typical calibration TOF spectrum for a helium beam. Oxygen, carbon and hydrogen are sputtered.

STEP 2

$$C_i^{H^-} = C_i^H + \sum_{k>i}\alpha_{ik}^{H^-H}C_k^H + \sum_{k\geq i}\alpha_{ik}^{H^-O}C_k^O \xrightarrow{\alpha_{ik}^{H^-O}<0.05} C_i^H = C_i^{H^-} - \sum_{k>i}\alpha_{ik}^{H^-H}C_k^H$$

$$\rightarrow J_i^H = \frac{C_i^H}{G_{ik}^{H^-H}E_i} \rightarrow \log J_i = a_0 + a_i \log E_i \qquad C_i^{H^-} = C_i^H + C_{k=4}^{He} + \sum_{k>i}\alpha_{ik}^{H^-H}C_k^H + \sum_{k\geq i}\alpha_{ik}^{H^-O}C_k^O$$

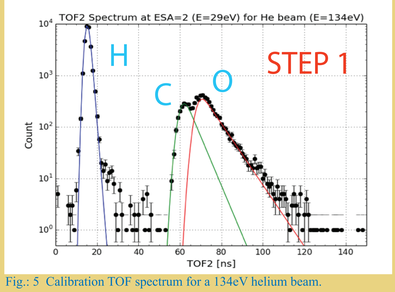

Fig.: 5 Calibration TOF spectrum for a 134eV helium beam.

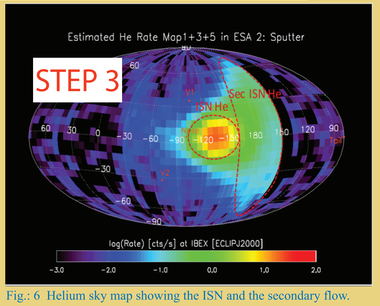

Fig.: 6 Helium sky map showing the ISN and the secondary flow.

Using the formula below and the calibration one can determine the real signal from the helium ENA's. With this procedure we generated the helium sky map as shown in figure 6 for energy step #2. One can see the ISN helium flow and the secondary component.

HELIUM ENA's AT: 1 AU & 150 AU

In order to determine the helium signal as seen at 150AU in the ISN flow direction we rotate the sky map and trace the ENA measure at 1AU to 150AU using the gravitational potential. The energies and pixel intensities are determined accordingly. The results is shown in figure 8.

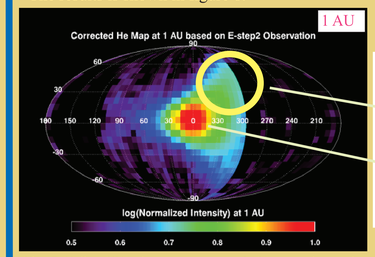

Fig.: 7 Helium ENA sky map measure at 1AU centered around the ISN flow

Secondary Component

Primary ISN

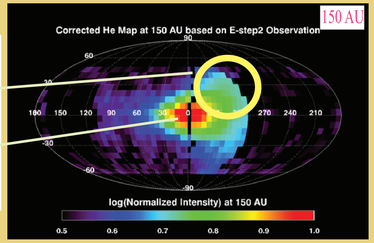

Fig.: 8 Helium ENA sky map at 150AU. The yellow circle show the secondary component.

$$\ddot{x}(t) = \frac{1}{m}F[x(t),\dot{x}(t),t], \qquad \dot{x}(t) = v(t), \qquad F = -\frac{GmM}{r^2}$$

ENA FLUX IN VARIOUS SECTORS IN THE 3D HELIOSPHERE (ASYMMETRIES):

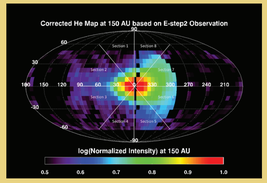

Fig.: 9 Sectors selected to investigate asymmetries.

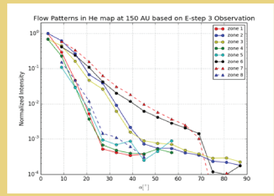

Fig.:10 Integrated and normalized intensity vs angle/distance for e-step 3 (52 eV) .

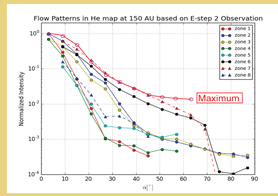

Fig.:11 Integrated and normalized intensity vs angle/distance for e-step 2 (27 eV).

ENA FLUX: THEORETICAL APPROACH

- Devide maps into sectors/orientation and apporximate flow arround an ellipsoidal obstacle with different aspect ratio l/d:

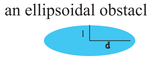

- Assume pressure balance
- Calculate plasma flow (subsonic & irrotational)

$$2c^2\nabla^2\boldsymbol{\varphi} = \nabla\boldsymbol{\varphi}\bullet\nabla\left(\nabla\boldsymbol{\varphi}\bullet\nabla\boldsymbol{\varphi}\right)$$

- Calculate flux:

$$\mathbf{j}(\boldsymbol{\Omega}) = \int_{R_{HP}}^{\infty} dr \frac{\sigma N_p n_{H_0^-}(\mathbf{x})}{4\pi} \int_{v_r<0} d^3\mathbf{v}\,\left|\mathbf{v_p}(\mathbf{x}) - \mathbf{V_0}\right| \left(\frac{m}{2\pi kT_p}\right)^{3/2} \exp\left[-\frac{kT_p}{m}\left(\mathbf{v} - \mathbf{v_p}(\mathbf{x})\right)^2\right]$$

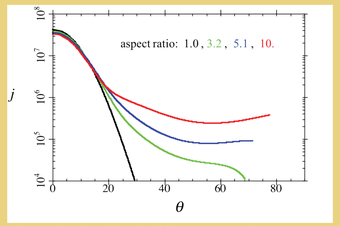

Fig.:12 Predicted flux for different aspect ratios -- curvature.

CONCLUSIONS:

- Oxygen and Helium ENA's show a secondary component. Statistical methods confirm the signal.
- After corrections for sputtered components and following trajectories from 1AU to 150 AU we generated helium ENA maps that are centered to the flow direction of the interstellar material.
- We the sectored these maps in eight equally spaced slices and determined the measured intensity as a function of angle away from the inflow center.
- There are clearly asymmetries in the all the sectors. The highest asymmetry is found in the direction of the secondary ENA component (sector 7) and its opposite direction (sector 3).
- **Measurements and theoretical predictions do NOT favour a symmetric model such as Opher et al. 2015.**